Available online at www.sciencedirect.com

ScienceDirect

Mendeleev Commun., 2020, **30**, 734–737

Mendeleev Communications

New PIM-1 copolymers containing 2,3,6,7-anthracenetetrayl moiety and their use as gas separation membranes

Igor I. Ponomarev,[a] Kirill M. Skupov,[a] Konstantin A. Lyssenko,[b] Inesa V. Blagodatskikh,[a] Alexander V. Muranov,[a] Yulia A. Volkova,[a] Dmitry Yu. Razorenov,*[a] Ivan I. Ponomarev,[a] Liudmila E. Starannikova,[c] Denis A. Bezgin,[c] Alexander Yu. Alentiev[c] and Yuri P. Yampolskii[c]

[a] *A. N. Nesmeyanov Institute of Organoelement Compounds, Russian Academy of Sciences, 119991 Moscow, Russian Federation. E-mail: razar@ineos.ac.ru, gagapon@ineos.ac.ru*
[b] *Department of Chemistry, M. V. Lomonosov Moscow State University, 119991 Moscow, Russian Federation*
[c] *A. V. Topchiev Institute of Petrochemical Synthesis, Russian Academy of Sciences, 119991 Moscow, Russian Federation*

DOI: 10.1016/j.mencom.2020.11.015

New PIM-1 copolymers with 2,3,6,7-anthracenetetrayl moiety have been synthesized as fine powders from 2,3,6,7-tetrahydroxy-9,10-di(*p*-fluorophenyl)anthracene monomer in DMSO, with crystal structure of the monomer as well as its precursors and the product of its model side crosslinking reaction being determined using X-ray diffraction. The microporosity and surface characteristics of the copolymers powders have been measured. As-cast membrane from the copolymer with 5 mol% of the monomer synthesized revealed promising gas separation properties as compared with original PIM-1.

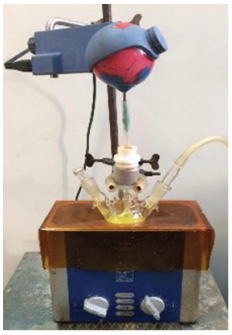

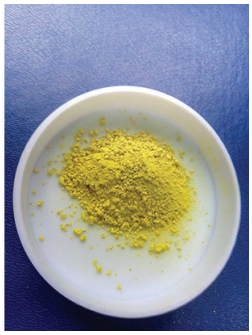

Keywords: gas separation membrane, ladder polymer, polymer synthesis, copolymer, micropores, PIM-1, sonochemistry, BET.

Polymers of intrinsic microporosity (PIMs) represent non-cross-linked soluble organic polymers with micropores originated from distorted packing of macromolecular chains. PIMs were synthesized for the first time by Budd and McKeown and have attracted considerable attention since 2004 due to their remarkable gas separation properties.[1–5] The most investigated PIM representative is a partially ladder spiroindanobenzodioxin polymer known as PIM-1, which is formed from commercially available 2,3,5,6-tetrafluoroterephthalonitrile (TFTPN) and 5,5′,6,6′-tetrahydroxy-3,3,3′,3′-tetramethylspiro-1,1′-bisindane (TTSBI). In the last 15 years many efforts have been applied to improve the PIM-1 gas separation performance as well as to address its physical aging and plasticization. One of possible solutions consists in selection of co-monomers for poly-condensation, which affects polymer chain conformation and thus membrane microporosity and morphology.[6] A lot of

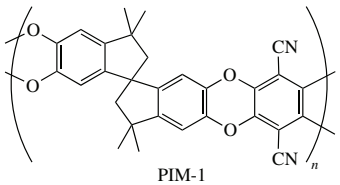

PIM-1

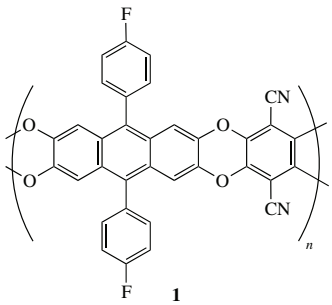

1

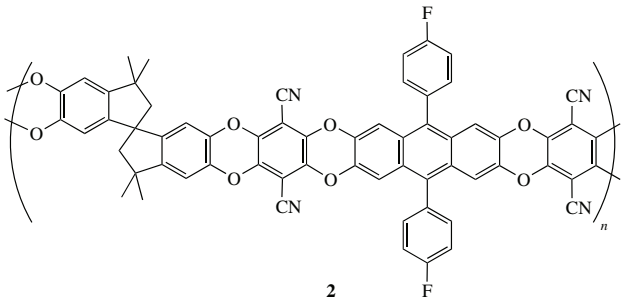

2

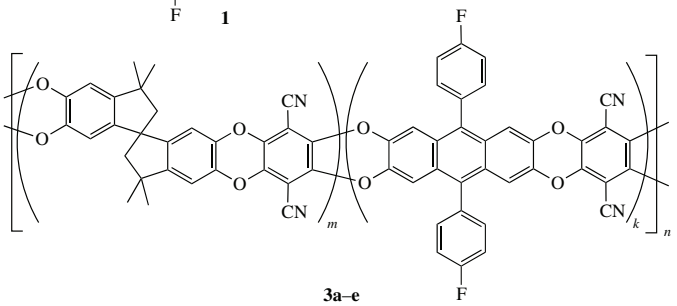

3a–e
(see Table 1)

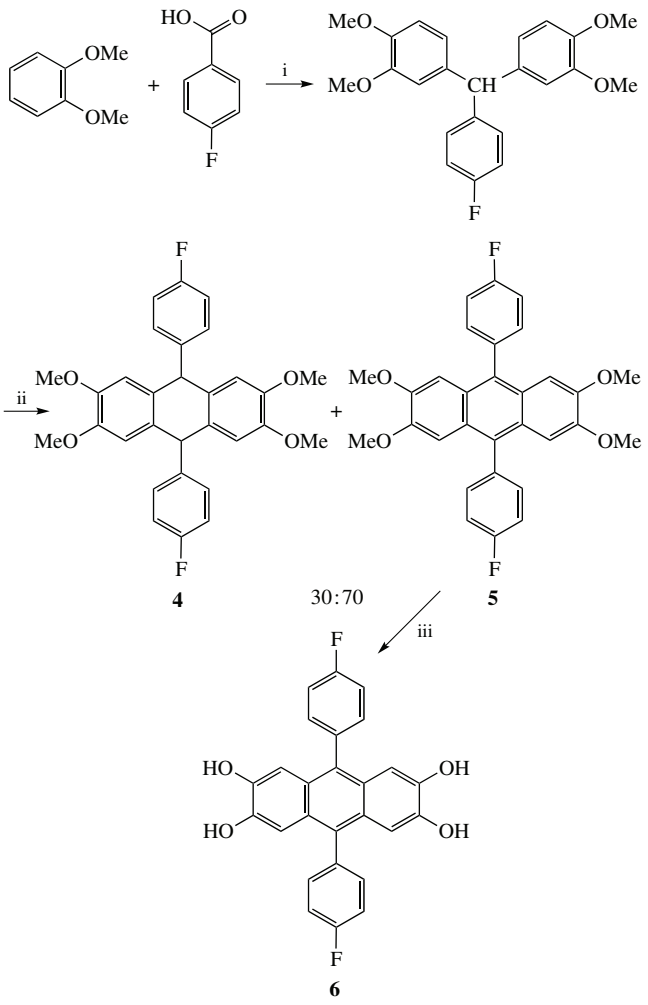

Scheme 1 *Reagents and conditions*: i, $H_3PW_{12}O_{40}$, MW, 5 min; ii, *p*-fluorobenzaldehyde, Ac_2O, $H_3PW_{12}O_{40}$, 90 °C, 2 h; iii, aq. HBr, AcOH, reflux, 6 h.

different tetrahydroxy-aromatics have been introduced into the PIM-1 synthesis instead of some structural parts of TTSBI.[1,2] However, only in few cases the polymers obtained demonstrated improved selectivity for several gas pairs compared with PIM-1.[7]

In this work, PIM-1 analogues **1–3** were synthesized starting from 2,3,6,7-tetrahydroxy-9,10-di(4-fluorophenyl)anthracene as a new monomer.

The monomer was obtained from veratrole and *p*-fluorobenzaldehyde using the known method[8] (Scheme 1).

Reaction of veratrole with substituted benzaldehyde was carried out in two steps. First, after 3–5 min under 120 W microwave irradiation in a household oven in the presence of phosphorus–tungsten heteropolyacid (HPA), the corresponding triphenylmethane derivative was generated (for details, see Online Supplementary Materials). This intermediate reacted with another portion of aldehyde, HPA and acetic anhydride resulting in relatively stable 2,3,6,7-teramethoxy-9,10-di(4-fluorophenyl)-9,10-dihydroanthracene **4** as by-product and the desired 2,3,6,7-tetramethoxy-9,10-di(4-fluorophenyl)anthracene **5** with a molar ratio of 30 : 70 in 70% total yield. Structures of compounds **4** and **5** were confirmed using NMR and X-ray diffraction (Figure 1).†

† *Crystal data for* **4**. $C_{30}H_{26}F_2O_4$, M = 488.53, monoclinic, space group $P2_1/c$, T = 120 K, a = 13.349(3), b = 5.4211(10) and c = 32.210(6) Å, β = 95.504(5)°, V = 2320.2(8) Å^3, Z = 4, Z' = 1, d_{calc} = 1.398 g cm^{-3}, μ(MoKα) = 1.02 mm^{-1}, F(000) = 1024. 21285 reflections were collected (5597 independent reflections, R_{int} = 0.1591) and used in the refinement, which converged to wR_2 = 0.1734, GOF = 0.915 for all independent reflections [R_1 = 0.0633 for 2472 reflections with $I > 2\sigma(I)$]. $2q_{max}$ was 56° (completeness 100%). Residual electron density 0.342/–0.327 e Å^{-3}.

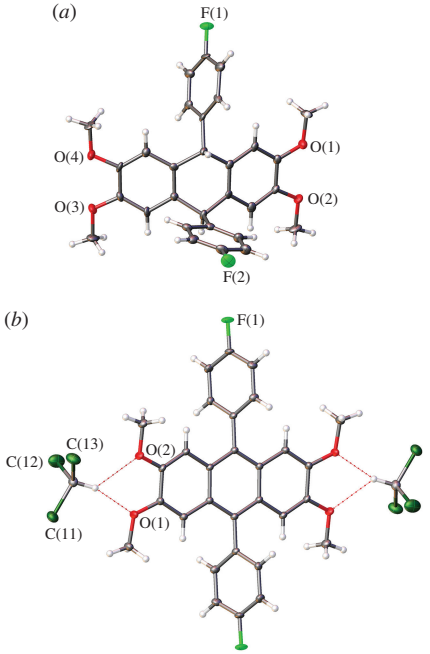

Figure 1 Molecular structures of compounds (*a*) **4** and (*b*) **5**·2$CHCl_3$. Displacement ellipsoids are drawn at 50% probability level.

Compound **4** spontaneously transformed in chloroform solution in air into fully aromatic derivative **5**, which was crystallized as a corresponding solvate. The X-ray data obtained were indispensable to a conformation analysis of the PIM-1 copolymers based on tetrahydroxyanthracene moiety because, for example, dihydro derivative **4** was not planar. By demethylation of tetramethyl ether **5**, 2,3,6,7-tetrahydroxy-9,10-di(4-fluorophenyl)anthracene **6** was obtained and its structure was also confirmed by X-ray data (Figure 2). Polycondensation

Crystal data for **5**·2$CHCl_3$. $C_{32}H_{26}Cl_6F_2O_4$, M = 725.27, triclinic, space group $P\bar{1}$, T = 120 K, a = 5.7424(4), b = 11.0710(8) and c = 13.0250(10) Å, α = 96.4190(10), β = 93.0650(10) and γ = 97.0720(10)°, V = 814.70(10) Å^3, Z = 1, Z' = 0.5, d_{calc} = 1.478 g cm^{-3}, μ(MoKα) = 5.75 mm^{-1}, F(000) = 370. 9827 reflections were collected (4318 independent reflections, R_{int} = 0.0173) and used in the refinement, which converged to wR_2 = 0.0879, GOF = 1.018 for all independent reflections [R_1 = 0.0323 for 3865 reflections with $I > 2\sigma(I)$]. $2q_{max}$ was 58° (completeness 100%). Residual electron density 0.613/–0.643 e Å^{-3}.

Crystal data for **6**·4Me_2CO. $C_{38}H_{40}F_2O_8$, M = 662.70, monoclinic, space group $P2_1/n$, T = 120 K, a = 14.2580(4), b = 7.9447(2) and c = 15.1400(4) Å, β = 93.2002(11)°, V = 1712.32(8) Å^3, Z = 2, Z' = 0.5, d_{calc} = 1.285 g cm^{-3}, μ(MoKα) = 0.96 mm^{-1}, F(000) = 700. 178050 reflections were collected (11030 independent reflections, R_{int} = 0.0690) and used in the refinement, which converged to wR_2 = 0.1713, GOF = 1.032 for all independent reflections [R_1 = 0.0522 for 7880 reflections with $I > 2\sigma(I)$]. $2q_{max}$ was 81° (completeness 100%). Residual electron density 0.625/–0.409 e Å^{-3}.

Crystal data for **7**. $C_{54}H_{12}F_{30}O_4$, M =1294.64, triclinic, space group $P\bar{1}$, T = 120 K, a = 5.8796(9), b = 11.363(2) and c = 18.586(3) Å, α = 99.456(4), β = 93.980(3) and γ = 99.719(3)°, V = 1201.2(3) Å^3, Z = 1, Z' = 0.5, d_{calc} = 1.790 g cm^{-3}, μ(MoKα) = 1.92 mm^{-1}, F(000) = 638. 13056 reflections were collected (9827 independent reflections, R_{int} = 0.0205) and used in the refinement, which converged to wR_2 = 0.0958, GOF = 1.030 for all independent reflections [R_1 = 0.0359 was calculated for 3865 reflections with $I > 2\sigma(I)$]. $2q_{max}$ was 55° (completeness 100%). Residual electron density 0.309/–0.344 e Å^{-3}.

CCDC 1991888–1991891 contain the supplementary crystallographic data for this paper. These data can be obtained free of charge from The Cambridge Crystallographic Data Centre *via* http://www.ccdc.cam.ac.uk.

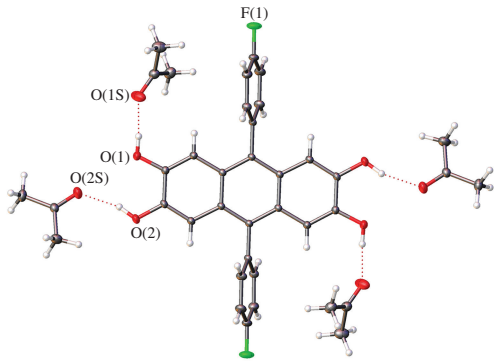

Figure 2 Molecular structure of compound **6**·4Me_2CO. Displacement ellipsoids are drawn at 50% probability level.

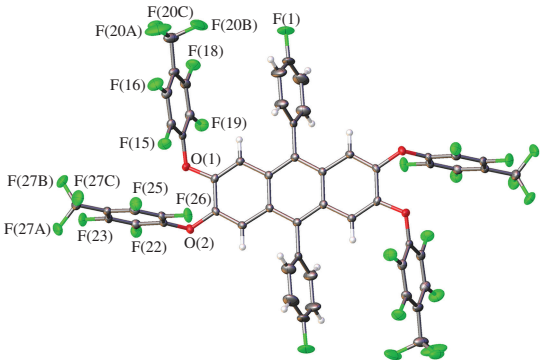

Figure 3 Molecular structure of compound **7**. Displacement ellipsoids are drawn at 50% probability level.

of monomer **6** with TFTPN in DMA or DMSO in the presence of K_2CO_3 was performed by the known methods[9,10] and resulted in formation of ladder polymer **1**, which was not soluble even in strong inorganic acids like methanesulfonic or sulfuric ones. An attempted approach to copolymer of compound **6**, TFTPN and TTSBI at the TTSBI to monomer **6** ratio (*m*/*k*) of 1 : 1 led again to fully insoluble product **2**. The insolubility of polymers **1** and **2** precluded a membrane casting and hence the intended application of these compounds.

In general, the hydroxyl groups in monomer **6** can react either coherently, resulting in dibenzodioxin cycles, or independently, producing branched and/or crosslinked structures. The latter way was confirmed by reaction of compound **6** with fourfold excess of perfluorotoluene as a highly active compound suitable for aromatic nucleophilic substitution. Complete reaction at all four hydroxyl groups of monomer **6** resulted in 9,10-bis(4-fluorophenyl)-2,3,6,7-tetrakis[2,3,5,6-tetrafluoro-4-(trifluoromethyl)phenoxy]anthracene **7**, whose structure was confirmed by NMR and X-ray analysis (Figure 3).

Thus, the mixed reactivity of 2,3,6,7-tetrahydroxyanthracenes in aromatic nucleophilic substitution with TFTPN and in their triple copolycondensation with TTSBI was verified. Therefore, we changed the copolymer synthesis strategy and the monomer loading scheme towards soluble high-molecular weight products with elevated content of PIM-1 units. The best outcome was obtained when the mixture of TTSBI and monomer **6** was pretreated with K_2CO_3 at room temperature for 0.6–1 h, which led to their activated deprotonated forms. Further addition of TFTPN and heating to 80 °C for 5 h in DMSO with ultrasonication (37 kHz) resulted in completely soluble high-molecular weight copolymers of TFTPN and compound **6**, namely products **3a**–**d**, with TTSBI–monomer **6** ratios (*m*/*k*) of 95 : 5, 90 : 10, 85 : 15 and 80 : 20, which had the reduced viscosity η_{red} values in 1,1,2,2-tetrachloroethane (TCE) of 0.70–0.81 dl g^{-1} and other physical properties collected in Table 1.

PIM-1 and its copolymers represent microporous materials, therefore special attention has been paid to investigation of their microporosity by surface analysis. Adsorption and desorption isotherms for polymers PIM-1 and **3a**–**d** are shown in Figures S8–S12 (see Online Supplementary Materials). These isotherms do not coincide for adsorption and desorption processes, which is typical of a microporous material. The values of total specific surface area S_{sp} calculated according to BET are similar (849–866 m^2 g^{-1}) for polymers PIM-1 and **3a**–**c** with 0–15% of monomer **6** and then drops when the incorporation of compound **6** reaches 20%, being 750 m^2 g^{-1} (see Table 1). The micropore specific surface area values S_{micro} were obtained according to the *t*-method. Copolymer **3a** with 5% of monomer **6** has higher S_{micro} value than pure PIM-1, namely 411 *vs*. 394 m^2 g^{-1}, which can be explained by the PIM-1 microstructure disruption by low amount of monomer **6**. Further increase in the monomer **6** incorporation, namely to 10, 15 and 20%, lowers the S_{micro} values up to 364 m^2 g^{-1} due to different packing pattern of the polymer chains. Polymers **3e** and **2** with 30 and 50% of monomer **6** incorporation, respectively, demonstrate a further decrease in the S_{micro} values. External surface area S_{ext} obtained by the *t*-method and related to meso- and macropores, is similar to the BJH surface area for pores with diameter $d > 2$ nm, which confirms reliability of the methods applied. BJH pore size distribution (Figures S8–S12) for a pore diameter range of 2–10 nm in the copolymers differs from that attributed to PIM-1, which allows one to assume that gas diffusion properties for the copolymers with anthracene moieties will also be different compared with those for PIM-1. To confirm this assumption, as-cast films of polymer **3a** (5% of monomer **6**) with the highest micropore specific surface area value were obtained from $CHCl_3$ and explored by gas chromatography,‡ resulting in the following preliminary data on the gas permeability (in Barrer): 1133 (He), 2985 (H_2), 1493 (O_2), 633 (N_2), 10338 (CO_2) and 1387 (CH_4). These values can be compared with the ones for as-cast PIM-1

Table 1 Physical properties of the synthesized copolymers.

Polymer	Ratio of TTSBI : **6** units (*m*/*k*)	η_{red}[a]/dl g^{-1}	M_W/kDa (GPC)	PDI (GPC)	S_{sp}[b]/m^2 g^{-1} (BET)	S_{micro}/m^2 g^{-1}	S_{ext}/m^2 g^{-1}	S/m^2 g^{-1} (BJH)	V_{sp}/cm^3 g^{-1}
PIM-1	100 : 0	1.17	120	3.8	856	394	463	424	0.575
3a	95 : 5	0.81	86.6	3.6	866	411	455	439	0.631
3b	90 : 10	0.76	80.6	3.3	849	394	455	423	0.598
3c	85 : 15	0.70	47.6	4.3	861	370	491	441	0.667
3d	80 : 20	0.70	38.2	4.0	750	394	386	346	0.618
3e	70 : 30	insoluble	–	–	829	350	478	453	0.604
2	50 : 50	insoluble	–	–	605	351	254	240	0.374

[a] η_{red} is reduced viscosity measured at 25 °C for 0.5 g dl^{-1} solutions in TCE for PIM-1 and **3a**,**b** or 0.25 g dl^{-1} solutions in TCE–CF_3COOH (97 : 3) for **3c**,**d**. [b] S_{sp}, S_{micro}, S_{ext} and S are total specific surface area according to BET, micropore specific surface area, external surface area and surface area according to BJH, respectively, measured for polymer powders after drying at 150 °C and residual pressure of 10^{-5} bar.

film, namely 760 (He), 1630 (H_2), 580 (O_2), 180 (N_2), 4390 (CO_2) and 310 (CH_4), obtained using the same equipment under the same experimental conditions.[11]

In summary, this work demonstrates a new approach to the synthesis of PIMs. The increase in gas permeability originating from the presence of 5 mol% monomer **6** can be attributed to the 2,3,6,7-anthracenetetrayl moieties that engage the statistically distributed extended ladder parts in the polymer structure. Another reason is the 4-fluorophenyl substituents, which are known to increase the permeability.[12] Further investigation of gas permeation and selectivity for this type of copolymers is planned.

This work was supported by the Russian Foundation for Basic Research (project no. 18-08-00472 A). Elemental analysis was supported by the Ministry of Science and Higher Education of the Russian Federation and was carried out using the equipment of 'Center for Molecular Composition Studies' of the A. N. Nesmeyanov Institute of Organoelement Compounds, Russian Academy of Sciences.

Online Supplementary Materials

Supplementary data associated with this article can be found in the online version at doi: 10.1016/j.mencom.2020.11.015.

‡ Permeability coefficients were determined with respect to He, H_2, O_2, N_2, CO_2 and CH_4 for the prepared films using gas chromatographic method at 20–22 °C. A steady state stream of tested gas at 1 atm contacted with the inlet surface of a film, while the penetrated stream was diluted by the carrier gas (typically He or alternatively N_2 when permeation of He or H_2 was measured). Partial pressure of the penetrant gases below the films was negligible compared with atmospheric pressure above the films. The permeability coefficients were calculated from the response of the thermal conductivity detector and an estimation for the stream flow.

References

1 Z.-X. Low, P. M. Budd, N. B. McKeown and D. A. Patterson, *Chem. Rev.*, 2018, **118**, 5871.
2 N. B. McKeown, *Sci. China: Chem.*, 2017, **60**, 1023.
3 P. M. Budd, E. S. Elabas, B. S. Ghanem, S. Makhseed, N. B. McKeown, K. J. Msayib, C. E. Tattershall and D. Wang, *Adv. Mater.*, 2004, **16**, 456.
4 P. M. Budd, B. S. Ghanem, S. Makhseed, N. B. McKeown, K. J. Msayib and C. E. Tattershall, *Chem. Commun.*, 2004, 230.
5 Y. Wang, X. Ma, B. S. Ghanem, F. Alghunaimi, I. Pinnau and Y. Han, *Mater. Today Nano*, 2018, **3**, 69.
6 I. I. Ponomarev, K. A. Lyssenko, D. Yu. Razorenov, Yu. A. Volkova, Iv. I. Ponomarev, K. M. Skupov, Z. S. Klemenkova, L. E. Starannikova, A. Yu. Alentiev and Yu. P. Yampolskii, *Mendeleev Commun.*, 2019, **29**, 663.
7 D. Fritsch, G. Bengtson, M. Carta and N. B. McKeown, *Macromol. Chem. Phys.*, 2011, **212**, 1137.
8 I. Mohammadpoor-Baltork, M. Moghadam, S. Tangestaninejad, V. Mirkhani, K. Mohammadiannejad-Abbasabadi and H. R. Khavasi, *Eur. J. Org. Chem.*, 2011, 1357.
9 I. I. Ponomarev, I. V. Blagodatskikh, A. V. Muranov, Yu. A. Volkova, D. Yu. Razorenov, Iv. I. Ponomarev and K. M. Skupov, *Mendeleev Commun.*, 2016, **26**, 362.
10 H. R. Kricheldorf, N. Lomadze, D. Fritsch and G. Schwarz, *J. Polym. Sci., Part A: Polym. Chem.*, 2006, **44**, 5344.
11 P. M. Budd, N. B. McKeown, B. S. Ghanem, K. J. Msayib, D. Fritsch, L. Starannikova, N. Belov, O. Sanfirova, Y. Yampolskii and V. Shantarovich, *J. Membr. Sci.*, 2008, **325**, 851.
12 Yu. P. Yampolskii, N. A. Belov and A. Yu. Alentiev, *Russ. Chem. Rev.*, 2019, **88**, 387.

Received: 28th April 2020; Com. 20/6208